Proceedings of ASME Turbo Expo 2011
GT2011
June 6-10, 2011, Vancouver, British Columbia, Canada

GT2011-46225

ANALYSIS OF GAS TURBINE ROTATING CAVITIES: ESTIMATION OF ROTOR DISK PUMPED MASS FLOW RATE

Riccardo Da Soghe *, **Bruno Facchini, Luca Innocenti, Mirko Micio**
Energy Engineering Department "S.Stecco"
University of Florence
50139, via S.Marta 3, Florence, Italy
Tel: (+39)0554796618, Fax: (+39)0554796342
Email: riccardo.dasoghe@htc.de.unifi.it

ABSTRACT

The dependable design of secondary air system is one of the main tasks for the safety, reliability and performance of gas turbine engines. To meet the increasing demands of gas turbine design, improved tools in prediction of the secondary air system behaviour over a wide range of operating conditions are needed. A real gas turbine secondary air system includes several components, therefore its analysis is not carried out using a complete CFD approach. Usually, these predictions are performed using codes, based on simplified approach which allows to evaluate the flow characteristics in each branch of the air system requiring very poor computational resources and little calculation time. Generally the available simplified commercial packages allow to correctly solve only some of the components of a real air system and often the elements with a more complex flow structure cannot be studied; among such elements, the analysis of rotating cavities is very hard.

This paper deals with a design-tool developed at the University of Florence for the simulation of rotating cavities. This simplified in-house code solves the governing equations for a steady one-dimensional axysimmetric flow using experimental correlations both to incorporate flow phenomena caused by multidimensional effects, like heat transfer and flow field losses, and to evaluate the circumferential component of velocity. The simplified calculation tool was designed to simulate the flow in a rotating cavity with radial outflow both with a Batchelor and/or Stewartson flow structures. Several studies have been carried out by the authors to develop suitable correlations for the discs friction coefficients and for co-rotation factor evaluation. The results of these analyses are available in the literature. In the present paper the authors develop, using CFD tools, reliable correlation for rotor disk pumped mass flow rate and provide a full 1D-code validation comparing, due to a lack of experimental data, the inhouse design code predictions with those evaluated by CFD.

NOMENCLATURE

A	area	$[m^2]$
b	outer radius of disk	$[m]$
G	gap ratio s/r_{out}	$[-]$
$\dot{m}$	mass flow rate	$[kg \cdot s^{-1}]$
p	static pressure	$[Pa]$
r	radius	$[m]$
s	rotor-to-stator axial distance	$[m]$
v	velocity	$[m \cdot s^{-1}]$
$\dot{m}_{out,r}$	rotor disk pumped mass flow rate	$[kg \cdot s^{-1}]$

Non dimensional groups

C_w	non-dimensional flow rate	$\dot{m}/(\mu b)$

*Address all correspondence to this author.

C_p	local pressure coefficient	$\frac{p(r)-p(b)}{\frac{1}{2}\rho(\Omega b)^2}$
Span	non-dimensional radial extension	$\frac{r-r_{in}}{r_{out}-r_{in}}$
Re_ϕ	rotational Reynolds number	$(r_{out}^2\Omega\rho)/\mu$
x	non-dimensional radius	r/r_{out}

Subscript

out	referred to disk radius
p	pumped
r	radial
s	superimposed
cav	whole cavity
φ	circumferential

Greek

λ_{turb}	turbulent flow parameter	$C_w/Re_\varphi^{4/5}$
β	core-swirl ratio, $\omega\backslash\Omega$	$[-]$
β^*	β without superposed flow	$[-]$
Δ	difference	$[-]$
μ	dynamic viscosity	$[Pa\cdot s]$
ρ	density	$[kg\cdot m^{-3}]$
Ω	angular speed of the rotor	$[rad\cdot s^{-1}]$

Acronym

CFD	Computational Fluid Dynamics

INTRODUCTION

The turbulent flow inside rotating cavities has been investigated for some decades because of its relevance in turbomachinery design and application. Generally, cooler high-pressure purge air bled from the compressor is injected into the cavities; a part or all of this air is ejected back into the main gas path annulus through the gap between disk rim seals. Accomplishing the cavity sealing and metal cooling using the smallest possible amount of purge air is a key objective in turbine design since the bleed-off of compressor air and its subsequent mixing with the main gas flow exact penalties on turbine performance. First studies on the isothermal flow structure in rotating disk systems were performed at the beginning of the past century. The historical controversy due to Batchelor (1951) and Stewartson (1953) is, in fact, well known [1]. The first specified the formation of a non-viscous core in the solid body rotation, confined between the two boundary layers which develop on the disks, while the latter found that the tangential velocity of the fluid can be zero everywhere apart from the rotor boundary layer. Later, Daily and Nece [2] noticed that the flow structure can be divided into four regimes, laminar and turbulent, with or without separated boundary layers. Few results have been published regarding rotor-stator systems with superimposed throughflow. Some authors [3] measured the average velocity profiles in the case of rotor-stator systems with a centrifugal imposed throughflow. Moreover, the authors showed that the flow parameter λ_{turb} is the similarity parameter of the turbulent flow that can be used directly to calculate the core-swirl ratio. Later, Kurokawa and Toyokura [4] proposed a 1D model to calculate the core-swirl ratio and the pressure distribution within the cavity, and introduced a coefficient of throughflow rate based on the rotating disk velocity. The authors validated the model by using experimental measurements. In a subsequent article [5] the same model was reviewed in order to allow its use for rotating cavity with narrow axial gap. In another article [6] the author solved the linear Ekman-layer equations for the case of a rotor-stator system with a superimposed radial outflow of fluid. The predicted rotational speed of the core between the boundary layers on the rotor and stator agrees well with published experimental measurements [3] when the super-imposed flow rate is zero, but the theoretical solutions underestimate the core rotation when the flow rate is non-zero. Details concerning the solution of the turbulent momentum-integral equations for the rotor to provide an approximation for the core rotation are also provided in the most comprehensive monograph of the state of understanding the flow and heat transfer processes in rotating disk systems [1]. More recently, a certain number of articles devoted to the development and/or validation of analytical models for core-swirl ratio prediction are available in literature. Among those, some papers are particularly interesting [7–11]. In the first four papers [7–10], the authors noticed that the equation that links β to the flow rate coefficient is according to a $5/7$ power law profiles, while in the last article [11] a new analytical law based on a $5/4$ power law profile is presented. In two of the above cited papers [7, 8], the analytical law has been validated by using extensive pressure and velocity measurements, for different values of the interdisk gap and in a large range of Reynolds numbers and flow rates. The measurements are obtained in water for a turbulent Batchelor type of flow, by means of a laser Doppler anemometer. Experimental results performed at the same test rig in a wide range of Reynolds numbers and flow rates, in the presence of inward and/or outward throughflow, have been also used to validate an advanced second-order turbulence model [8–12]. The excellent agreement of numerical predictions with the velocity and pressure measurements confirmed that the described RSM turbulence model is a valuable tool for flow analysis in rotor-stator systems. Other authors focused their investigations on the application of standard turbulence models in solving swirled flow in rotating cavities [13–15]. In the first paper [13], the authors presented a CFD benchmark performed for closed cavity flow with rotor-stator, contra-rotating and co-rotating disks. The authors tested several turbulence models and compared numerical predictions with measurements of an experimental test case: k-ω Shear-Stress Transport SST model performed the best agreement. In another article [14] the authors focused their works on the comparison of CFD predictions obtained with a two-equation k-ω SST turbulence model with experimental measurements carried out by hot-wire anemometry and three-holes pressure probe. The authors reveal that the experiments are qualitatively well described by numerical results. Also in the last paper cited [15], the authors performed a CFD campaign by simulating the turbulence with the k-ω SST model. This selection was based on a survey of turbulence models in a two-dimensional, axisymmetric CFD analysis for a shrouded rotor-stator cavity with the disk walls at different speeds. Compared to measured velocity profiles the k-ω SST model demonstrated the best overall agreement. Recently Da Soghe et al. have performed a numerical benchmark of turbulence modeling in a gas turbine rotor-stator system [16]. The authors compared their CFD predictions with the experimental data provided by Poncet and co-workers [7, 9, 11]. The authors point out that the k-ω SST well predicts the experimental results. This paper deals with a design-tool developed at the University of Florence for the simulation of rotating cavities. A detailed description of the in-house code is given in some recently published articles [17–20] together with the discussion of the results obtained in a preliminary code testing campaign. Those results showed that the 1D code is able to provide fairly accurate predictions about fluid-dynamics quantities trends but it was also pointed out that the program showed some discrepancies, with respect to 3D CFD data, as the overall pressure growth is accurately predicted. Those discrepancies, in principle, could be addressed both to the correlations used to evaluate the core-swirl ratio and the mass flow rate pumped by the rotor disc. In the past the authors focused on the co-rotation factor prediction and some useful correlations were developed [17, 19].

On the other hand, an accurate and reliable rotor disk pumped mass flow rate prediction plays a fundamental role in a rotor-stator system analysis. The present study is focused on the rotor disk pumped mass flow rate evaluation. The analysis is limited to a simple two faced discs cavity, without shrouds, with an axial gap so large that a core region sets in. The rotor disk pumped mass flow rate is predicted by applying the theoretical correlation proposed by Owen and Rogers [1] inserted in the 1D in-house code. CFD predictions led the authors to review the correlation in order to minimize the revealed discrepancies.

IN-HOUSE CODE STATOR-ROTOR CAVITIES ROTOR DISK PUMPED MASS FLOW RATE EVALUATION

A detailed description of the in-house code is given some already published articles [17, 18] together with the discussion of the results obtained in a preliminary code testing campaign. With regards to the rotor disk pumped mass flow rate evaluation, in the present work the authors performed an exhaustive and detailed study using the following experimental correlation proposed by Owen [6]:

$$\frac{\dot{m}_o}{\mu r} = \varepsilon_m (x^2 Re_\varphi)^{4/5} \tag{1}$$

where:

$$\varepsilon_m = \frac{49\pi}{60}\alpha\gamma|1-\beta|^{8/5} \tag{2}$$

α and γ parameters could be expressed as a function of β [1, 6].

Rearranging this equation, it is possible to define the radius where the rotor pumped mass flow rate is equal to the superposed one:

$$C_w = \varepsilon_m Re_\varphi^{4/5} x^{13/5} \tag{3}$$

thus:

$$x = \left(\frac{\lambda_{turb}}{\varepsilon_m}\right)^{5/13} \tag{4}$$

Owen and Rogers [1] pointed out that in case of free disk the ε_m is equal 0.219, while it assumes lower values when β is different from zero (i.e. the rotating disk in a rotating fluid). The last statement means that, referring to the correlation proposed in [1, 6], the transition from Stewartson to Batchelor flow type takes place for $\lambda_{turb} x^{-13/5}$ values lower than 0.219.

TESTED GEOMETRY AND SIMULATIONS CONDITION

The analyzed geometry consists in a simple plane faced discs rotor-stator cavity.

Table 1. Geometrical dimensions of tested cavity

Parameters	
$r_{out} \backslash r_{in}$	7.50
$s \backslash r_{out}$	0.13

The cavity dimensions are quoted in table 1. The gap ratio G value was selected in order to assure that separate boundary layers exist. Such very simple configuration allowed to perform a full test of the monodimensional model in terms of localization of the core region, assessment of rotor disk pumped massflow rates and, finally, pressure rise across the cavity. Furthermore this kind of geometry fits very well with the purpose of the development of correlations from CFD data.

Table 2. Tested operative conditions

	Parameters
C_w	$7 \cdot 10^3 - 2 \cdot 10^4$
λ_{turb}	$0.09 - 0.2$

The non-dimensional flow parameters ranges considered for the present analysis are quoted in table 2. The computations' boundary conditions in terms of rotor disk angular speed and coolant massflow rate were determined using a full factorial non-dimensional flow parameters distribution. The number of levels for the λ_{turb} are 6 while 4 levels were used for the C_w.

The selected λ_{turb} values enable the development of a core region within the wheel space region, in order to perform a detailed evaluation of one-dimensional program capabilities in predicting the growth of a recirculation region and its radial localization. To this purpose all simulations were performed in adiabatic conditions in order to avoid the superpositions of heat transfer effects in this phase of correlations testing. The numerical tests were conducted in a quiescent environment, thus no blades and vanes were modeled. Thus the external peripheral asymmetries have not been considered in this work. The last statement does not represent a restriction: equation 1 just estimate the rotor disk pumping mass flow rate and may be used only to quantify the internally induced ingestion rate. So this correlation is always applicable to evaluate the rotor disk pumped flow, even in case of externally induced ingestion due to the presence of external peripheral asymmetries. Finally, reference to a stator-rotor cavity is not a limiting aspect: in fact, the correlation for the estimation of the rotor disk pumped mass flow rate is always applicable even in case of different co-rotation factor pattern as in other kind of rotating cavities.

CFD COMPUTATIONS

CFD steady state calculations were performed with the commercial 3D Navier-Stokes solver CFX-10.0. All numerical simulations were performed with 5° sector model (figure 1). As already discussed, the numerical analysis here reported focuses on the inner cavities flow, so the flowpath was not included in the computations. Periodicity was imposed at the sectors circumferential boundaries while no-slip and adiabatic conditions were

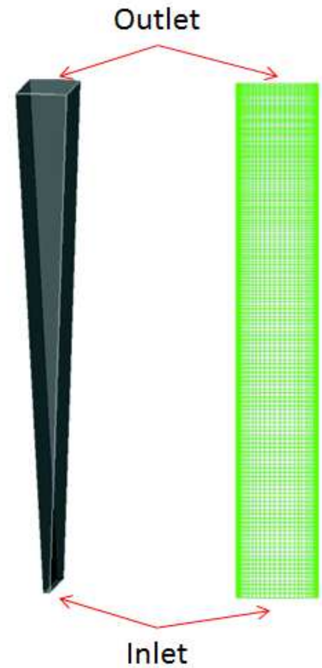

Figure 1. Computational domain and grid

applied on solid surfaces. A pressure boundary condition was imposed at the outlets while mass flow rates were imposed at the inlets. No swirl have been imposted at the inlet. Compressibility effects were taken into account and *High Resolution* advection schemes were used. The fluid was modeled as ideal gas and the properties of specific heat capacity, thermal conductivity and viscosity were assumed as a function of temperature.

The energy equation was solved in terms of total temperature and viscous heating effects were accounted for.

Following the suggestion of both Roy et al. [15] and Da Soghe [17, 21], the k-ω SST turbulence model, in its formulation made available by the CFD solver, was used in conjunction with a low Reynolds approach.

The mesh generation tool ICEM CFD was used to generate a hexahedral cells mesh. A number of grid sensitivity tests were conducted in order to ensure mesh independence solutions. The final mesh dimension, in terms of number of elements, is around 60k cells (figure 1).

The convergence of solutions was assessed by monitoring the torque on the cavities walls, the mass flow through the outlet and residuals.

CFD RESULTS

A first validation of CFD computations was performed comparing our numerical predictions with the published experimental and numerical data (Daily et. al [6] and Da Soghe et al. [21]).

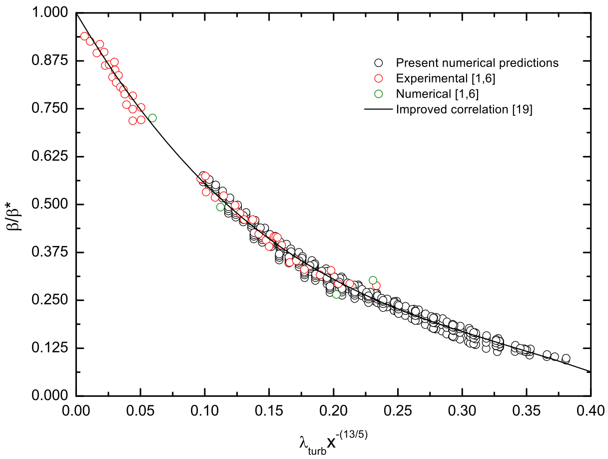

Figure 2. CFD β predictions

As shown in figure 2, the agreement within the common range, in terms of core-swirl ratio versus the local flow rate coefficient , is good. As the co-rotation factor is strictly related to the transition from the Stewartson to the Batchelor flow type (and then with the rotor disk pumped mass flow rate), it can be assumed that a confident evaluation of the tangential velocity leads to a reliable evaluation of rotor disc pumped mass flow rate. Within the chosen non-dimensional flow parameters range (table 2), all CFD calculations predicted quite a similar flow structure.

As an example, figure 3 shows the distribution of β/β^* and $v_r/(\Omega r)$ obtained for $C_w = 16730$ and $\lambda_{turb} = 0.09$. It is clearly evident that at the inlet of the cavity the tangential velocity of the fluid is zero everywhere apart from the rotor boundary layer and the centrifugal throughflow fills the whole axial gap between the disks. However, in the upper region of the calculation domain, a rotating core confined between the two boundary layers develops.

The two flow structures, described above, are separated by a transition region that, in this case, fills a wide portion of the cavity. Starting from the entry of the calculation domain, that region is characterized by a sharp reduction of the radial velocity component and by a slight rise of the circumferential one (figure 4). The Stewartson flow type can be recognized by the absence of the rotating core, while the Batchelor flow structure is revealed by the strong increase of β/β^*. In the whole computation domain the radial velocity component behaves inversely to the circumferential one (figure 3). With regards to the radial localization of the transition region, for all of CFD runs the beginning of the core region can be defined for $\lambda_{turb}x^{-13/5}$ values higher than 0.22 (figure 4).

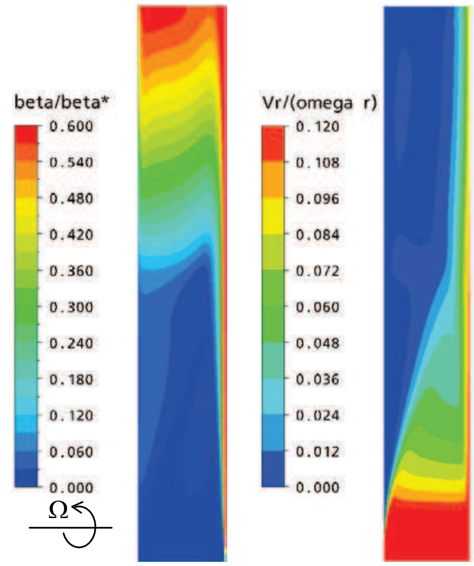

Figure 3. CFD results: β/β^* and $Vr/(\Omega r)$ contour ($C_w = 16730$, $\lambda_{turb} = 0.09$)

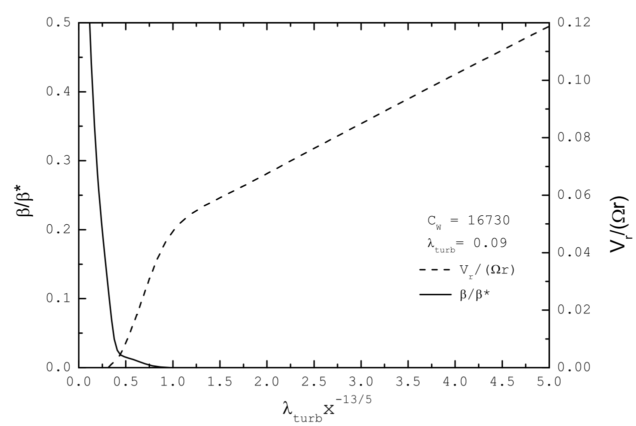

Figure 4. CFD results: β/β^* and $Vr/(\Omega r)$ profile ($C_w = 16730$, $\lambda_{turb} = 0.09$)

The last statement is confirmed by figures 5 and 6. In these figures the dotted line represents the cavity outflow mass flow rate that exceeds the superimposed one. To point out the mentioned profile, this parameter was evaluated on a number of isosurfaces at constant radius in accordance with the following expression:

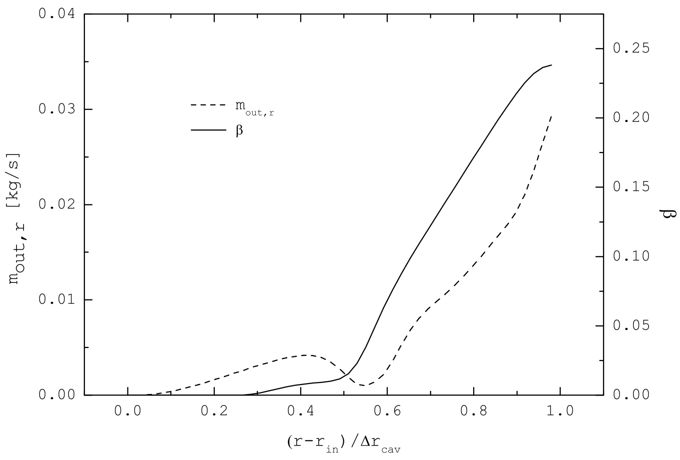

Figure 5. $\dot{m}_{out,r}$ and β over radius (C_w=16730, λ_{turb}=0.09)

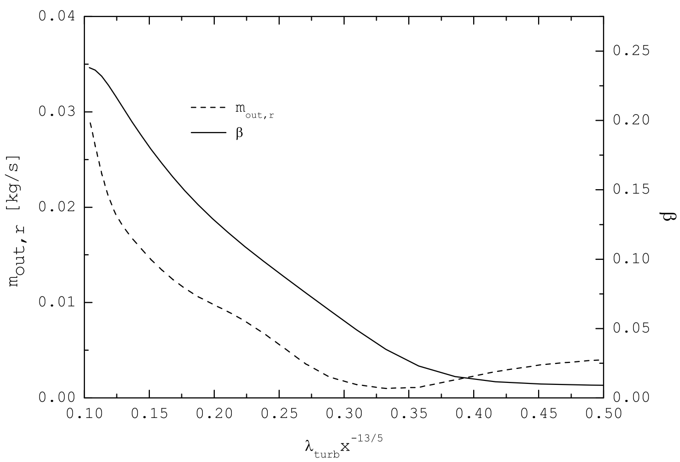

Figure 6. $\dot{m}_{out,r}$ and β over $\lambda_{turb}x^{\frac{-13}{5}}$ (C_w=16730, λ_{turb}=0.09)

$$\dot{m}_{out,r} = \frac{1}{2}\left(\int_{A,r} \rho \|v_r\| dA - \dot{m}_s\right) \tag{5}$$

where A,r represent the generic iso-surface at a constant radius. Referring to figure 5, the increase of the $\dot{m}_{out,r}$ parameter at the lower radii can be motivated by the presence of the inner vortex shown in figure 7. After that votex, $\dot{m}_{out,r}$ drops close to zero and then takes off as the core region takes place. As shown in figure 6, the $\dot{m}_{out,r}$ profile takes off (i.e. the core region starts), for $\lambda_{turb}x^{\frac{-13}{5}}$ higher than 0.219 confirming that CFD predicts a higher rotor disk pumped mass flow rate with respect to Owen and Roger's correlation. This evidence is true for all tested conditions reported in this paper.

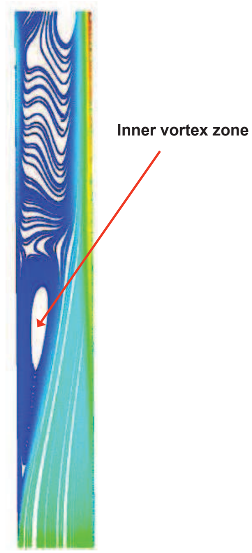

Figure 7. Cavity inner vortex: 2D streamlines

Improved Correlation

In order to improve the correlation proposed by Owen in [6], the authors focused on the product $\alpha \cdot \gamma$.

In [4, 5] the authors expressed this term as a function of the rotational Reynolds number while Owen has correlated α and γ as functions of the co-rotation factor β. Rearranging the expressions 1 and 2 as follows,

$$\alpha \cdot \gamma = \frac{\dot{m}_0}{\mu r}\frac{60}{49\pi}\frac{1}{|1-\beta|^{8/5}}\frac{1}{\left(x^2 \mathrm{Re}_\varphi\right)^{4/5}} \tag{6}$$

CFD data have been used in order to evaluate the dependencies of the $\alpha \cdot \gamma$ term by Re_φ and β. From this analysis it emerges that the fundamental parameter for the $\alpha \cdot \gamma$ term evaluation is the co-rotation factor. The expression that better correlates the CFD data was found in the following form (figure 8):

$$\alpha \cdot \gamma = A\beta^2 + B\beta + C \tag{7}$$

where $A,,$ are equal, respectively, to 0.9433, -0.6116, 0.1766 (figure 8) to be used in the ranges C_w $7 \cdot 10^3 - 2 \cdot 10^4$, λ_{turb} $0.09 - 0.2$.

The discrepancies between the CFD data and the whole cavity rotor disk pumped mass flow rate evaluated by the use of the improved correlation 7, are shown in figure 9.

The obtained correlation provides the rotor disk pumped mass flow rate with an accuracy below 10%.

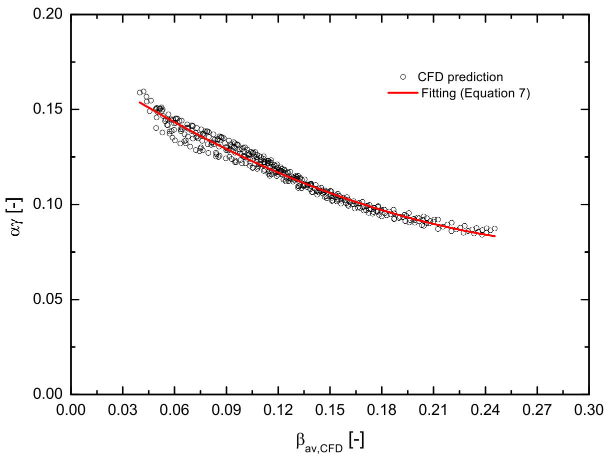

Figure 8. $\alpha \cdot \gamma$ versus β

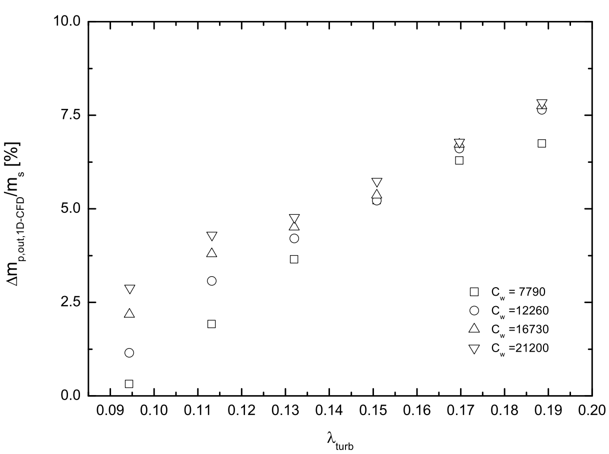

Figure 9. Rotor disk pumped mass flow rate: correlation accuracy

Combining equations 1 and 2, it is possible to correlate the co-rotation factor with the $\lambda_{turb} x^{\frac{-13}{5}}$ parameter. That relationship results in a curve that represents the locus of points such that the superimposed mass flow rate is equal to the rotor disk pumped rate (figure 10). The co-rotation factor and the $\lambda_{turb} x^{\frac{-13}{5}}$ are also linked by the Daily universal curve [19]. The $\lambda_{turb} x^{\frac{-13}{5}}$ value is such that the the two mentioned curves intersect each other, which represents the transition point from source to core region (figure 10).

Consistent with figure 6, using the developed correlation

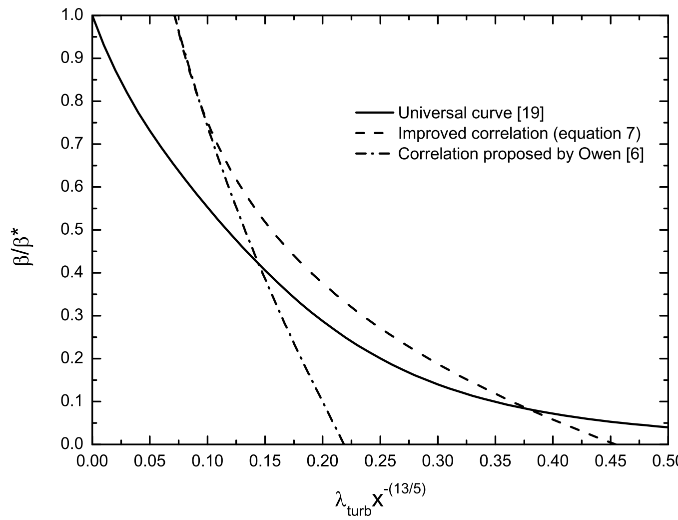

Figure 10. Transition from Stewartson to Batchelor flow type

(equation 7), the Batchelor flow type sets in for $\lambda_{turb} x^{\frac{-13}{5}}$ equal to 0.35.

1D MODEL PREDICTIONS

The 1D in-house program has been tested in detail, under the same calculation conditions as in the CFD analysis. In order to appropriately compare its predictions with the 3D calculations, the authors chose to perform some comparisons in terms of rotor disk pumped mass flow rate and local pressure coefficient C_p, defined in the following equation:

$$\mathrm{C}_p = \frac{p(r) - p(b)}{\frac{1}{2}\rho(\Omega b)^2} \tag{8}$$

Figure 11 shows the rotor disk pumped mass flow rate in case of $\lambda_{turb} = 0.09$. From that figure it emerges that the improved correlation developed here, provides an accurate evaluation of the rotor disk pumped mass flow rate if compared with CFD predictions.

The correlation proposed by Owen [6], as already discussed, estimates a lower pumped mass flow rate as the transition from the source to the core region occurs at higher radii. It could also be pointed out that, according to those remarked above, no significant changes occur for different values of C_w parameter.

The effects of the λ_{turb} parameter on the cavity flow field is shown in figure 12. Consistent with this theory, the increase of the λ_{turb} parameter leads to a redaction of the core region extension. Even if the improved correlation inserted in the 1D code correctly predicts the cavity flow types transition radius for all tested conditions, as the λ_{turb} increases the discrepancies between CFD data and $1D$ predictions rise. This last issue does not represent a limiting factor because in the case of wide source region the ingested mass flow rate values are quite low if compared with the superimposed ones (see figure 9). With regards to the behaviour of the correlation originally proposed by Owen [6], its usage in $1D$ code leads to a strong over estimation of the source region extension that results in an absence of the core region in the case of high λ_{turb} values. Figure 13 and 14 show the local pressure coefficient versus the radial span, predicted by CFD computations and by the 1D program, using both the improved correlation (equation 7) and that of Owen [6]. In particular, the results concerning four different C_w values for the same λ_{turb} are plotted in figure 13 . The authors want to stress how the improved correlation proposed shows a better agreement of 1D predictions with CFD computation, in terms of local pressure distribution. The results shown in figure 14, concerning the six different λ_{turb} for the same value of C_w, confirm what the authors noticed above. For all analyzed cases, it is possible to recognize a Stewartson flow type at the lower radius, where the diffusive effect is dominant due to the increase of the cross-section (heavier near the inlet of the cavity) and a Batchelor flow type where the pressure rises strongly due to the increase of the tangential velocity.

Effect of the nondimensional flow rate The increase of the nondimensional flow rate for a given turbulent flow parameter (figure 13) does not significantly modify the flow field that develops in the cavity. Particularly, the radial extension of the Batchelor flow type region remains unchanged as the whole pressure rise. It is indeed well known that the pumping magnitude only depends on the turbulent flow parameter [1].

Effect of the turbulent flow parameter The increase of the turbulent flow parameter for a given nondimensional flow rate (figure 14) reduces the radial extension of the Batchelor flow region. Evidence of this effect is the shift towards higher radial span values of the significant pressure rise. That phenomenon, already known in literature [1] [7] [11] , causes a reduction of the global cavity pumping. Finally, it should be pointed out how the increase of the λ_{turb} parameter for a given C_w coincides with a rotational Reynolds number decrease.

CONCLUSION AND PERSPECTIVE FOR FUTURE WORK

In their previous work [18], the authors concluded that their one-dimensional modeling approach estimates the shape of the radial profile of pressure and temperature in reasonably good agreement with CFD predictions, but the estimation of the overall pressure growth is unsatisfactory. This effect, was ascribed to the inaccurate β values prediction operated by the in-house code. The discrepancies, in principle, could be related to two distinct factors. The first one is the used correlations for the co-rotation factor evaluation. The second one is the rotor disk pumped mass-flow rate. Focusing on the first factor, the authors have developed some improved correlations for the β evaluation and the results of these works are available in open literature [17, 19].

In this paper the authors improve a well known correlation for the rotor disk pumped mass flow rate through an exhaustive CFD analysis focusing on a simple two faced discs cavity. The improved correlation was successfully implemented within the in-house code and the cavity solver program predictions were then compared with those related to the CFD ones in a wide range of operating conditions. The following main conclusions emerged. Using the improved correlation for the rotor disk pumped mass flow rate, the discrepancy of core-swirl ratio and cavity pressure rise profiles between the in-house code and CFD data is strongly reduced. This evidence emerges for all tested conditions and therefore we can conclude that significant improvements have been achieved.

ACKNOWLEDGMENT

The authors wish to thank Professor J. M. Owen or the helpful and the stimulating discussions.

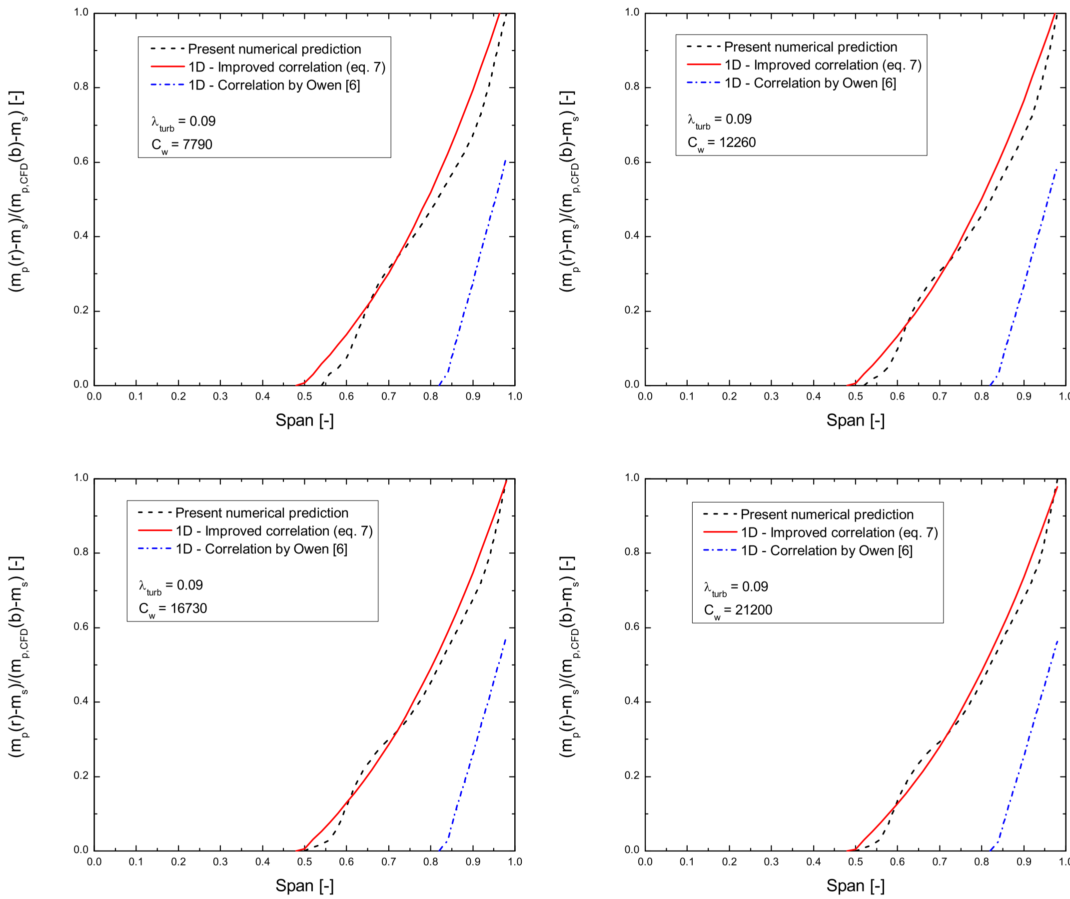

Figure 11. Rotor disk pumped mass flow rate vs radial span - $\lambda_{turb} = 0.09$

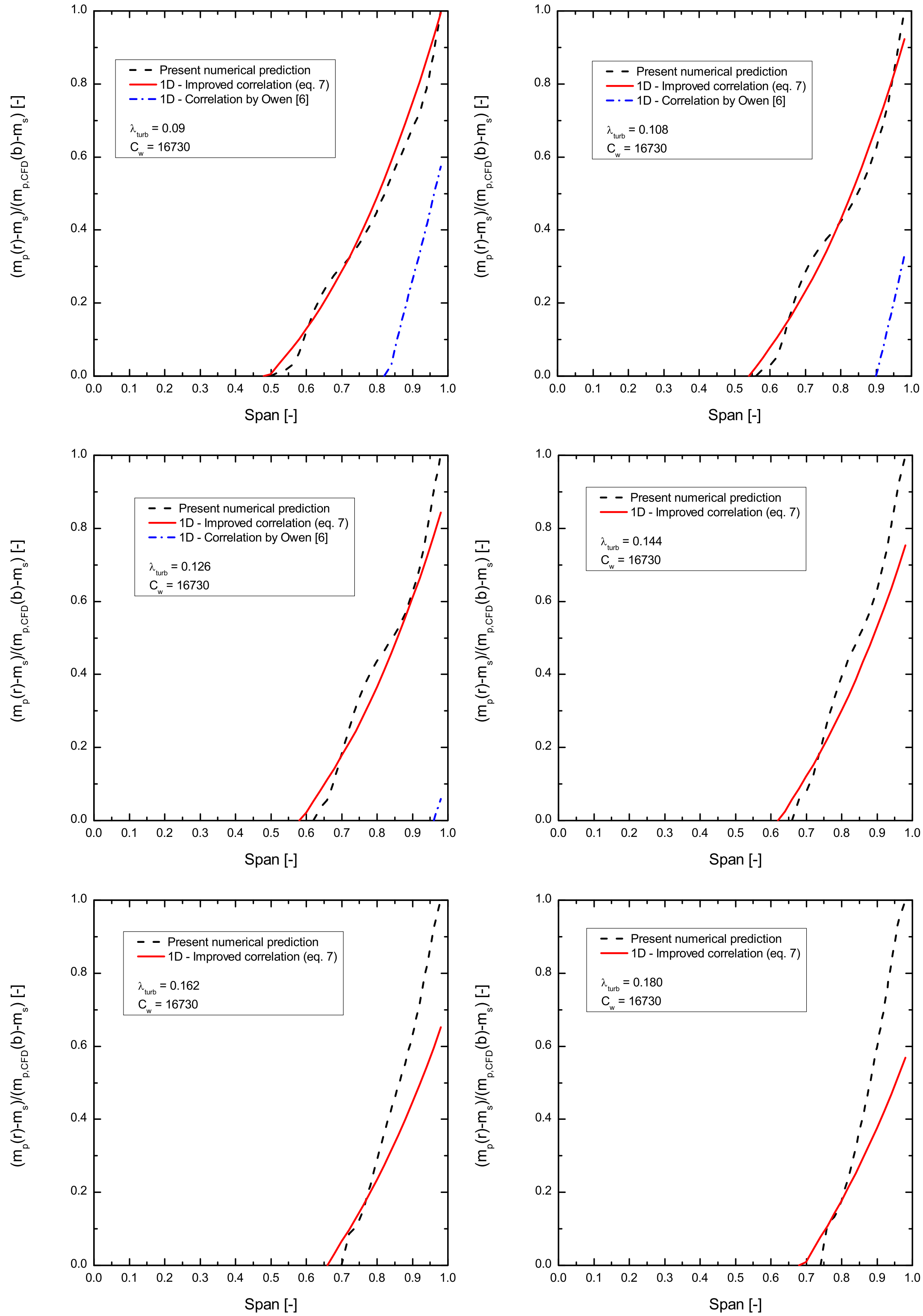

Figure 12. Rotor disk pumped mass flow rate vs radial span - $C_w = 16730$

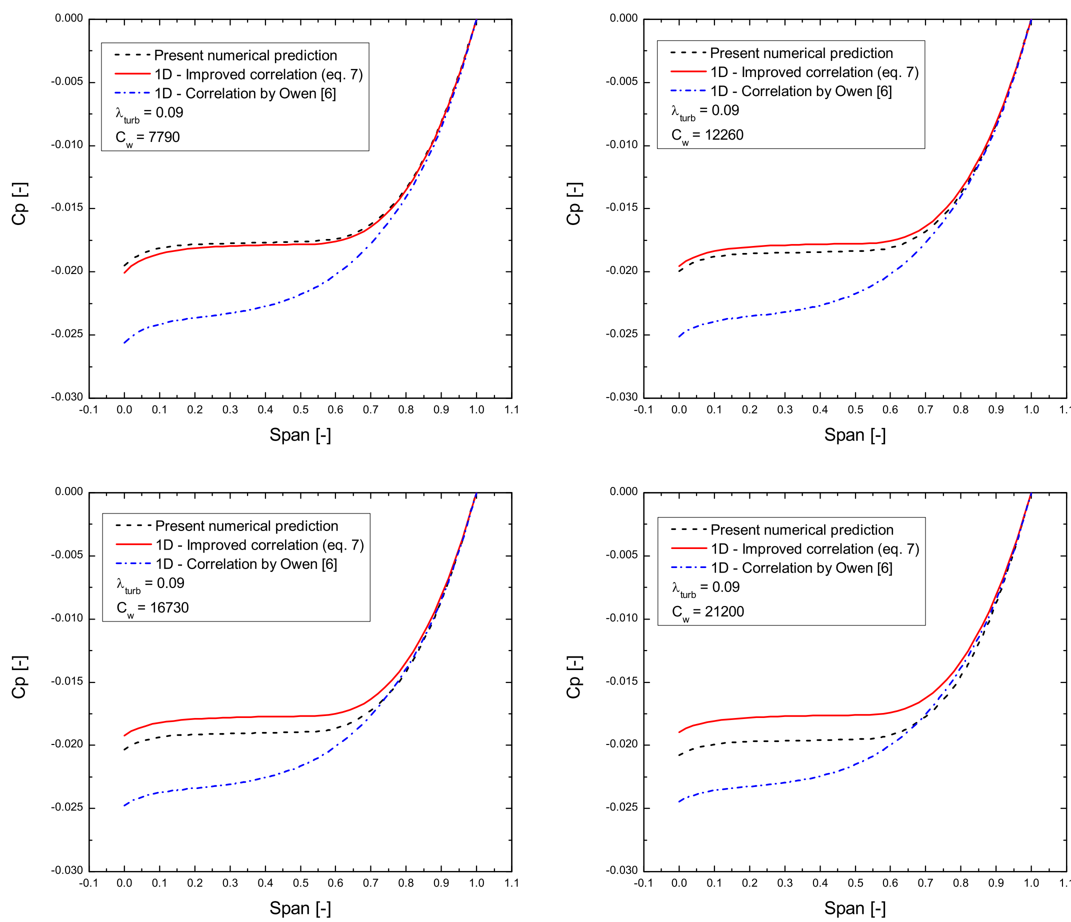

Figure 13. C_p vs radial span - $\lambda_{turb} = 0.09$

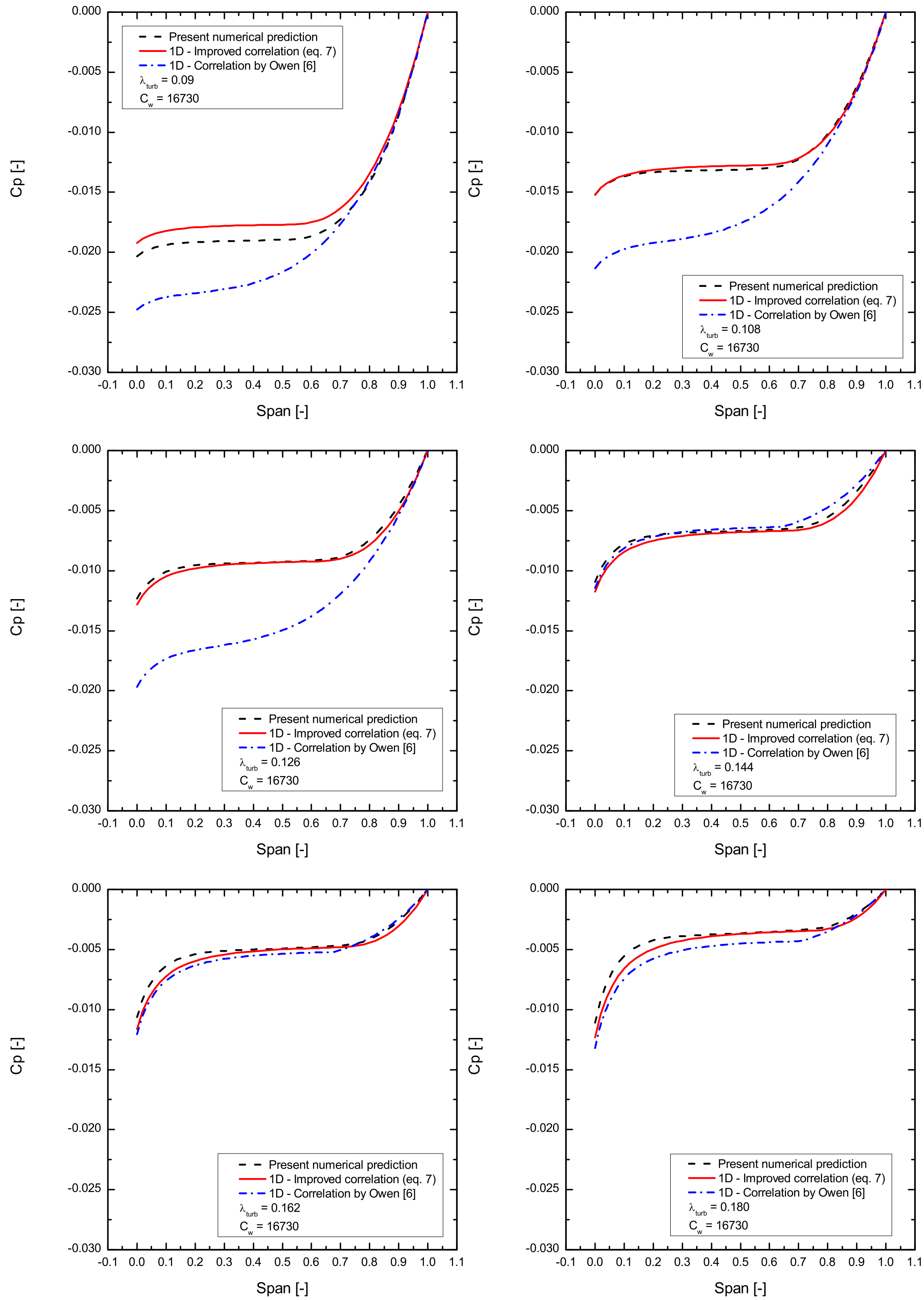

Figure 14. C_p vs radial span - $C_w = 16730$

REFERENCES

[1] Owen, J. M., and Rogers, R. H., 1989. *Flow and Heat Transfer in Rotating Disc Systems. Volume 1 - Rotor-Stator Systems*.

[2] Daily, J. W., and Nece, R. E., 1960. "Chamber dimension effects on induced flow and frictional resistance of enclosed rotating disks". *ASME J. Basic Eng,* **82**, pp. 217–232.

[3] Daily, J. M., Ernst, W. D., and Asbedian, V. V., 1964. "Enclosed rotating discs with superimposed throughflow". *Dept. of Civil Engineering Hydrodyin. Lab MIT. Rep. No. 64*.

[4] Kurokawa, J., and Toyokura, T., 1972. "Study on axial thrust of radial flow turbomachinery". *2nd International JSME Symposium Fluid Machinery and Fluidics*(Tokyo).

[5] Kurokawa, J., and Sakuma, M., 1988. "Flow in a narrow gap along an enclosed rotating disk with through-flow". *JSME Int. J.*(Ser. II, 31(2), pp. 243251).

[6] Owen, J. M., 1988. "An approximate solution for the flow between a rotating and a stationary disk". *ASME Paper*(88-GT-293).

[7] Poncet, S., Chauve, M. P., and Gal, P. L., 2005. "Turbulent rotating disk flow with inward throughflow". *J. Fluid Mech.,* **522**, pp. 253–262.

[8] S. Poncet, M. P. Chauve, P. L. G. "Study of the entrainment coefficient of the fluid in a rotor-stator cavity". *6th European Conference on Turbomachinery*(Fluid Dynamics and Thermodynamics Vol.1, p.246-256).

[9] Poncet, S., Schiestel, R., and Chauve, M., 2005. "Centrifugal flow in a rotor-stator cavity". *J. Fluids Engi.,* **127**, p. 787.

[10] Poncet, S., Chauve, M. P., and Schiestel, R., 2005. "Turbulence modelling and measurements in a rotor-stator system with throughflow". *Engineering Turbulence Modelling and Experiments*(vol. 6, pp.761-770).

[11] Poncet, S., Chauve, M. P., and Schiestel, R., 2005. "Batchelor versus Stewartson flow structures in a rotor-stator cavity with throughflow". *Phys. Fluids,* **17**(7).

[12] R. Debuchy, S. Poncet, F. A., and Bois, G., 2009. "Experimental and numerical investigation of turbulent air flow behaviour in a rotor-stator cavity". *ETC 8 paper*.

[13] Innocenti, L., Micio, M., Da Soghe, R., and Facchini, B., 2008. "Analysis of gas turbine rotating cavities by an one-dimensional model". *ISROMAC Paper*(12-2008-20161).

[14] Debuchy, R., Gatta, S. D., D'Haudt, E., Bois, G., and Martelli, F., 2007. "Influence of external geometrical modifications on the flow behaviour of a rotor-stator system: numerical and experimental investigation". *Proc. of the Institution of Mechanical Engineers, Part A: J. Power Energ.,* **221**(6), pp. 857–864.

[15] Roy, R. P., Zhou, D. W., Ganesan, S., Wang, C. Z., Paolillo, R. E., and Johnson, B. V., 2007. "The flow field and main gas ingestion in a rotor-stator cavity". *Asme Paper*(2007-GT-27671).

[16] Da Soghe, R., Innocenti, L., Andreini, A., and Poncet, S., 2010. "Numerical benchmark of turbulence modeling in gas turbine rotor-stator system". *ASME Paper*(GT2010-22627).

[17] Da Soghe, R., Innocenti, L., Micio, M., and Facchini, B., 2009. "Analysis of gas turbine rotating cavities by an one-dimensional model: Definition of a new discs friction coefficients correlation set". *ASME Journal of Turbomachinery*(1088, Press in progress).

[18] C. Wu, B. Vaisman, K. M., and Paolillo, R., 2006. "Cfd analysis prediction of heat transfer coefficient in rotating cavities with radial outflow". *ASME Paper*(GT2006-91078).

[19] Micio, M., 2011. "Gas turbine secondary air system: experimental analysis and design tools developing". *PhD Thesis*.

[20] Bianchini, C., Facchini, B., Da Soghe, R., Innocenti, L., Micio, M., Bozzi, L., and Traverso, S., 2008. "Development of numerical tools for stator-rotor cavities calculation in heavy-duty turbines". *ASME Paper*(2008-GT-51268).

[21] Da Soghe, R., S.Poncet, and L. Innocenti, A. A., 2010. "Numerical benchmark of turbulence modeling in gas turbine rotor-stator system". *ASME Turbo Expo*(GT2010-22627).